The AtRbx1 protein is part of plant SCF complexes, and its down-regulation causes severe growth and developmental defects

Esther Lechner, Daoxin Xie, Sandrine Grava, Emmanuelle Pigaglio, Séverine Planchais, James A.H. Murray, Yves Parmentier, Jérome Mutterer, Bertrand B. Dubreucq, Wen-Hui Shen, et al.

THE JOURNAL OF BIOLOGICAL CHEMISTRY
Vol. 277, No. 51, Issue of December 20, pp. 50069–50080, 2002

Printed in U.S.A.

The AtRbx1 Protein Is Part of Plant SCF Complexes, and Its Down-regulation Causes Severe Growth and Developmental Defects*

Received for publication, May 1, 2002, and in revised form, October 11, 2002
Published, JBC Papers in Press, October 14, 2002, DOI 10.1074/jbc.M204254200

Esther Lechner‡, Daoxin Xie§, Sandrine Grava‡, Emmanuelle Pigaglio‡, Severine Planchais¶, James A. H. Murray¶, Yves Parmentier‡, Jerome Mutterer‡, Bertrand Dubreucq‖, Wen-Hui Shen‡, and Pascal Genschik‡**

From the ‡Institut de Biologie Moléculaire des Plantes du CNRS, 12, rue du Général Zimmer, 67084 Strasbourg Cédex, France, the §Laboratory of Plant Signal Transduction, Institute of Molecular Agrobiology, National University of Singapore, Singapore 117604, Republic of Singapore, the ¶Institute of Biotechnology, University of Cambridge, Cambridge CB2 1QT, United Kingdom, and the ‖Laboratoire de Biologie des Semences, INRA-INAPG, Route de St-Cyr, 78026 Versailles, France

Recently in yeast and animal cells, one particular class of ubiquitin ligase (E3), called the SCF, was demonstrated to regulate diverse processes including cell cycle and development. In plants SCF-dependent proteolysis is also involved in different developmental and hormonal regulations. To further investigate the function of SCF, we characterized at the molecular level the *Arabidopsis* RING-H2 finger protein AtRbx1. We demonstrated that the plant gene is able to functionally complement a yeast knockout mutant strain and showed that AtRbx1 protein interacts physically with at least two members of the *Arabidopsis* cullin family (AtCul1 and AtCul4). AtRbx1 also associates with AtCul1 and the *Arabidopsis* SKP1-related proteins *in planta*, indicating that it is part of plant SCF complexes. *AtRbx1* mRNAs accumulate in various tissues of the plant, but at higher levels in tissues containing actively dividing cells. Finally to study the function of the gene *in planta*, we either overexpressed *AtRbx1* or reduced its expression by a dsRNA strategy. Down-regulation of *AtRbx1* impaired seedling growth and development, indicating that the gene is essential in plants. Furthermore, the AtRbx1-silenced plants showed a reduced level of AtCul1 protein, but accumulated higher level of cyclin D3.

The SCF complex(es) (named after the three original yeast protein subunits: Skp1, Cdc53 (cullin), and F-box proteins) belong to a class of ubiquitin ligase (ubiquitin-protein isopeptide ligase (E3))[1] required for the degradation of key regulatory proteins involved in cell cycle progression, development, and signal transduction (reviewed in Refs. 1–3). The F-box proteins are thought to be the adapter subunits that recruit specifically substrates to the core ubiquitylation complex through physical interaction between the F-box domain and the Skp1 subunit (4). For instance in budding yeast, the F-box protein Grr1p recruits the G_1 cyclins Cln1p and Cln2p via its leucine-rich repeats, whereas the Cdc4p F-box protein interacts with the Sic1p protein by WD40 repeats, leading to SCF-dependent ubiquitylation and subsequent degradation of the target substrates. In animal cells, SCF-dependent ubiquitylation also regulates the turnover of a number of cell cycle regulators and signaling proteins. The F-box protein SKP2 is involved in the turnover of the transcription factor E2F-1 (5) and the cyclin-dependent kinase inhibitor p27 (6), whereas hCDC4/Fbw7/Ago are involved in cyclin E protein degradation (7–9). β-TRCP is an F-box protein that interacts with phosphorylated IκBα and β-catenin proteins, thereby playing an important role in β-catenin/Tcf and nuclear factor κB-dependent signaling (10, 11).

The SCF complexes are also constituted by a fourth essential stoichiometric subunit named in yeast and animal cells Hrt1p/Rbx1p/Roc1p (12–15) and hereafter called Rbx1. The Rbx1 protein belongs to the ring finger domain RING-H2 protein family and plays a key function in stimulating the ubiquitylation reaction (reviewed in Ref. 16). The structure of the human quaternary SCF^{Skp2} complex (Cul1-Rbx1-Skp1-F-box^{Skp2}) has recently been achieved (17). A model has been proposed in which Cul1 is positioning the substrate via the F-box protein SKP2 in close proximity to the catalytic module consisting of Rbx1 and the ubiquitin-conjugating enzyme. Because Rbx1 interacts with both cullin and an ubiquitin-conjugating enzyme, it may thus serve as an allosteric activator of the later. Cullin proteins are also covalently modified by an ubiquitin-related protein called Need8/Rub1 (18, 19), and it has been shown that Rbx1 may be involved in this process (20). Mutation of *Rbx1* gene in budding yeast results in a cell cycle arrest before DNA replication, and the mutant is defective in degradation of Sic1 and the G_1 cyclin Cln2 (12, 14). Developmental and/or physiological consequences of *Rbx1* overexpression or depletion are poorly understood in higher eukaryotes.

In plants genetic studies have highlighted the important function of F-box proteins in a number of developmental and physiological processes. Both auxin and jasmonate perception are controlled, at least in part, by SCF-like complexes involving the F-box proteins Tir1 and Coi1, respectively (Refs. 21 and 22; reviewed in Refs. 23–25). Indeed, recently it was demonstrated that auxin stimulates the binding of the SCF^{Tir1} to the AUX/IAA proteins leading to their degradation (26). Furthermore mutants in the *Arabidopsis* F-box genes *UFO* (27); *ZTL*, *FKF1*, and *LKP2* (28–30); *EID1* (31); *ORE9* (32); and *SON1* (33)

* This work was supported by "Action Concertée Incitative Jeune Chercheur" from French Ministry of Research and by the French plant genomic program "Genoplante." The costs of publication of this article were defrayed in part by the payment of page charges. This article must therefore be hereby marked "*advertisement*" in accordance with 18 U.S.C. Section 1734 solely to indicate this fact.

** To whom correspondence should be addressed. Tel.: 33-3-88-41-72-78; Fax: 33-3-88-61-44-42; E-mail: pascal.genschik@ibmp-ulp.u-strasbg.fr.

[1] The abbreviations used are: E3, ubiquitin-protein isopeptide ligase; CDK, cyclin-dependent kinase; Dex, dexamethasone; dsRNA, double-stranded RNA; EST, expressed sequence tag; GFP, green fluorescent protein; GST, glutathione *S*-transferase; GUS, β-glucuronidase; PTGS, post-transcriptional gene silencing.

suggest that SCF-dependent ubiquitylation reactions are also involved in floral patterning, the regulation of circadian rhythm, phytochrome A-specific light signaling, natural and hormone-induced senescence processes, and defense responses to pathogen, respectively. *Arabidopsis* genome encodes almost 700 possible F-box proteins (34), suggesting that SCF-dependent proteolysis is a fundamental mechanism in plants regulating many developmental and cellular processes.

To further investigate the function of SCF in plants, we characterized at the molecular level *AtRbx1* from *Arabidopsis*. We found that the *AtRbx1* gene is able to functionally complement a yeast mutant strain. Furthermore, we demonstrate that AtRbx1 associates physically with at least two members of the *Arabidopsis* cullin family (AtCul1 and AtCul4) and two SKP1-like proteins (ASK1 and ASK2). RNA gel blots were performed to study the expression of the *AtRbx1* genes in various tissues of plants and after different stimuli. Finally, we used both inducible overexpression and dsRNA strategies to investigate the function of the gene *in planta*.

EXPERIMENTAL PROCEDURES

Unless stated otherwise, all procedures for manipulating DNA and RNA were carried out according to Refs. 35 and 36.

Chemicals—Dex (Sigma) was dissolved in ethanol and kept at a concentration of 30 mM.

Construction of Plasmids—Construct pTA::GFP is described in Ref. 37, and construct pTA::GUS was a gift from L. Lepiniec. To construct pTA::Rbx1, we used PCR-based site-directed mutagenesis to introduce *Xho*I and *Bam*H1 restriction sites upstream and downstream of the coding region of *AtRbx1;1* using oligonucleotide 5′-CGGGGTACCTCGAGAATGGCGACACTAGACTCCGACGTTACCATGATTCC-3′ and oligonucleotide 5′-GACTAGTGACCATATTTCTGAAACTCCC-3′, respectively. For gene silencing, AtRbx1 antisense and sense coding sequences were separated by a spacer sequence consisting of the GFP coding sequence. Thus to construct pTA::dsRNA-Rbx1, a *Bam*HI-*Spe*I GFP fragment, obtained by PCR, was first introduced in the pBluescript vector (Stratagene) resulting in plasmid pKS-GFP. *AtRbx1* coding region was introduced in antisense orientation upstream from the GFP by PCR amplification using oligonucleotide 5′-ATCTAGCTCGAGTGCGGTGGTAACCAAATGAAC-3′ and oligonucleotide 5′-ACTAGTGAATTCGCGACACTAGACTCCGACGT-3′ and using the *Xho*I and *Eco*RI restriction sites. To introduce *AtRbx1* coding region in sense orientation downstream the GFP, *AtRbx1* sequence was PCR-amplified using oligonucleotide 5′-TGATCATCTAGAGCGACACTAGACTCCGACGT-3′ and oligonucleotide 5′-TACGTTGAGCTCACTAGTTGCGGTGGTAACCAAATGAAC-3′, digested by *Xba*I and *Sac*I, and introduced into *Spe*I and *Sac*I restriction sites, resulting in construct pKS::dsRNA-Rbx1. The *Xho*I-*Spe*I DNA fragment, encoding the dsRNA-Rbx1 construct, was subcloned into the Dex-inducible vector pTA7002 (38), resulting in plasmid pTA::dsRNA-Rbx1.

To make *myc*-tagged ASK1 or ASK2, full-length ASK1 (At1g75950) or ASK2 (At5g42190) was PCR-amplified and fused in frame to the six copies of *myc* epitope into the plasmid pROK2 that contains cauliflower mosaic virus (CaMV) 35 S promoter in the binary vector pBIN19, resulting in p*myc*-ASK1 and p*myc*-ASK2.

Plant Material, Transformation, and Treatments—The *Arabidopsis* plants were of the Wassilewskija (Ws) ecotype. Seeds were produced under greenhouse conditions. Transgenic *Arabidopsis* plants were obtained by *Agrobacterium*-mediated transformation using the floral dip method (39, 40). Plants were grown on soil with 12-h day and 12-h night. *In vitro* plants were grown onto Murashige and Skoog medium M0255 (Dushefa) supplemented with 1% sucrose (conditions used: 16-h day at 20 °C and 8-h night at 17 °C). Dex was directly added at a concentration of 1 μM to the medium or sprayed onto plants in solution at 10 μM (with 0.01% Tween 20).

AtRbx1 expression in response to the plant hormone auxin was assayed according to Ref. 41. For the dark to light transition, *Arabidopsis* plants were grown *in vitro* in complete darkness for 12 days, and then transferred to standard light condition and collected after 1, 3, and 8 h. For heat shock, 14-day-old *Arabidopsis* plants grown *in vitro* under standard conditions were collected and incubated in sterile water either at 38 °C for the heat shock or at 22 °C for the control. After 90 min of treatment, plants were incubated in sterile water at 22 °C and collected 1 h later for RNA preparation. The leaf-strips experiments used to study *AtRbx1* expression during re-initiation of cell division activity in *Arabidopsis* have been described previously (42).

Histological Analysis—Cotyledons were sampled 10 and 22 days after germination. Plant materials were fixed and post-fixed at 4 °C in 100 mM phosphate buffer, pH 7.2, containing 1% glutaraldehyde and 0,1% OsO_4 and embedded in LR White™ resin (EMS, Fort Washington, PA; catalog no. 14380). 0.5-μm sections were prepared and stained with 1% (w/v) toluidine blue for morphological analysis or Lugol's reagent to check for starch accumulation. To visualize cotyledon epidermal cells, the cotyledon of 22-day post-germination seedlings of dsRNA-2 line were first cleared for chlorophyll by rinsing with ethanol (70–95%), than re-hydrated and finally incubated for 2 h in Hoyer's solution (chloral hydrate/gum arabic/glycerol/water (100:7.5:5:30 g)). Size and shape of cotyledon epidermal cells were analyzed by Nomarski optics on an E800 (Nikon) microscope and the images recorded with Sony DXC950 camera. Cell area measurements were performed on a Macintosh computer using the public domain ImageJ program (developed at the United States National Institutes of Health and available on the Internet at rsb.info.nih.gov/ij/).

RNA Gel Blotting and Semiquantitative RT-PCR—RNA gels were performed with 20 μg of total RNA/lane. The RNA extraction and RNA gel blotting procedures are described in Ref. 37. The AtRbx1;1 probe corresponds to the entire cDNAs clone. The histone H4 probe corresponds to the 196-bp restriction fragment *Acc*I-*Dde*I of the coding region of the gene *H4A748* (43). The *SAUR* probe corresponds to the PCR-amplified genomic fragment of the *SAUR-AC1* gene (41). The photosystem II W probe corresponds to cDNA clone FB025d05F (gene At4g28660). The clone used to perform HSP105/110 is described in Ref. 44. The integrity and the amount of RNA applied to each lane were verified by ethidium bromide staining and hybridization with a probe encoding the translation elongation factor 1-α (cDNA clone 232A19T7, gene At1g07920).

For semiquantitative RT-PCR, 2 μg of total RNA (treated with the DNase A) extracted from different *Arabidopsis* organs were used for cDNA synthesis using Moloney murine leukemia virus Retro Transcriptase RNase H^- (Promega) according to the recommendations of the supplier. To determine the expression of the two *AtRbx1* genes, PCR were performed using specific primers designed in the 3′-untranslated regions of both genes. For *AtRbx1;1*, a transcript of 269 nucleotides was amplified using primer 5′-CAGCAGATGGCTAAAGACTCGTCA-3′ and primer 5′-ACGTCACCCAAAGCACAACCATAA-3′, and for *AtRbx1;2* a transcript of 135 nucleotides was expected using primer 5′-CAGCAGATGGCTAAAGACTCGTCA-3′ and primer 5′-ATCTGCATCAAAGACATCCCAAGAGAAGA-3′. The PCR reactions were conducted using *Taq* polymerase (Invitrogen). To control the equal amount of matrix used for RT-PCR, a PCR, amplifying the constitutive expressed AtCul1 gene (45), was performed. A transcript of 242 nucleotides was amplified using primer 5′-TGGCCTGACATGCTTCCGTGA-3′ and primer 5′-TCCAGCTTGATGCCTTGCGAGA-3′. All the PCR reactions were performed with an annealing temperature of 58 °C for 40 s. After 24 cycles of PCR, 20 μl of the reaction was run on an 2% agarose gel. The amplified DNA was visualized by ethidium bromide staining and also transferred to a nylon membrane and probed with the corresponding random primed ^{32}P-labeled probes.

The method of extraction and visualization of the low molecular weight RNA is described in Ref. 46.

Overexpression and Purification of the AtRbx1-GST Fusion Protein and Pull-down Reactions—*Bam*HI and *Eco*RI sites were introduced on the 5′ and the 3′ side of the AtRbx1;1-coding sequence using PCR-based site-directed mutagenesis. The PCR reaction was performed using oligonucleotide 5′-CGCGGATCCTTAGTGACCATATTTCTGAAACT-3′ and oligonucleotide 5′-CCGGAATTCATGGCGACTCTAGACTCCGACGTTA-3′ as the upstream and downstream primers, respectively. The *Bam*HI-*Eco*RI fragment was cloned into the pGEX-2KT vector (Amersham Biosciences) for expression in the *Escherichia coli* strain BL21(DE3)pLysE. In the pGEX-2KT-Rbx1 construct, GST is placed in frame at the N terminus of the fusion protein. Low yield of the fusion protein was obtained after 4 h of 1 mM isopropyl-1-thio-β-D-galactopyranoside induction, but the fusion protein remained soluble and was thus purified in the native form under non-denaturing conditions on bulk glutathione-Sepharose 4B (Amersham Biosciences).

The GST pull-down assays were performed with 4 μg of purified GST or GST-Rbx1 fusion protein fixed to glutathione-Sepharose 4B resin (Amersham Biosciences) and incubated during 3 h at 4 °C with 2.5 mg of total protein extracts prepared from 2-week-old *Arabidopsis* seedlings. After two washing steps with PBS buffer (140 mM NaCl, 2.7 mM KCl, 10 mM Na_2HPO_4, 1.8 mM KH_2PO_4, pH 7.3), proteins were eluted with 1 ml of glutathione elution buffer (10 mM reduced glutathione in 50 mM Tris-HCl, pH 8). The eluted proteins were lyophilized overnight,

suspended in PBS, and desalted with PlusOne mini dialysis kit (Amersham Biosciences).

Protein Extraction, Preparation of Antibodies, and Immunoblotting—The *Arabidopsis* plants were homogenized using pestle and mortar in extraction buffer (25 mM Tris-HCl, pH 7.5, 15 mM $MgCl_2$, 15 mM EGTA, 150 mM NaCl, 0.1% Tween 20, 1 mM dithiothreitol, and complete protease inhibitor mixture mix (Roche Molecular Biochemicals)) with PolyClar AT (Serva) and quartz and centrifuged at 20,000 × *g*. The protein content was determined by using the Bio-Rad protein assay kit. Samples of 15 μg of proteins were separated by SDS-PAGE gels and transferred to Immobilon-P membrane (Millipore, Bedford, MA).

A peptide containing the C-terminal sequence (CPLDNSEWEFQKYGH) of AtRbx1;1 was synthesized, linked to keyhole limpet hemocyanin carrier proteins, and used to immunize rabbits. The antiserum was diluted 1:1500 for Western blot analysis. To detect the AtCul1 protein, we used the purified rabbit polyclonal anti-Cul1 antibody (45) diluted 1:4000. For protein loading control, we used a rabbit polyclonal antibody against the PSTAIRE epitope (Santa Cruz Biotechnology, Inc) at a dilution of 1: 1000. To detect the *myc*-tagged ASK1 or ASK2 proteins, we used the *myc* monoclonal mouse antibody (9E10) purchased from the Berkeley Antibody Co., at a dilution of 1:1000. To detect ubiquitin-protein conjugates, we used a commercial rabbit polyclonal antibody (catalog no. UG9510) purchased from Affinity Research Products Ltd. The antibody was used at a dilution of 1:1000. To detect cyclin D3, we used a rabbit polyclonal antiserum raised against the C-terminal peptide of the protein (47) at a dilution of 1:800. The immunoreactive proteins were detected using peroxidase-conjugated goat anti-rabbit antibodies (Dianova) and the ECL Western blot analysis system from Amersham Biosciences. Determination of the specificity of the antibodies was performed by competition experiments. In this case, the antibody was incubated for 3 h at room temperature without or with 1 μM antigen peptide before application to the membranes.

Immunoprecipitation of the SCF Complexes—1 mg of total protein extracted from wild type plants or plants expressing either the *myc*-tagged ASK1 or ASK2 was incubated with 100 μl of the anti-*myc* affinity matrix (Berkeley Antibody Co.) for 6 h at 4 °C with gentle rocking. The beads were then washed five times with the protein extraction buffer and eluted with 0.1 M glycine, pH 3.0. Eluted proteins were then resolved on SDS-PAGE and used for Western blot analysis.

Yeast Strain MCY557 Complementation—Budding yeast strain MCY557 (*MATα/MAT***a** *his3Δ200/his3Δ200 can1R/can1R ura3/ura3 leu2/leu2 trp1/trp1 lys2/lys2 RBX1/rbx1*::*HIS3*) (12) in which the *Rbx1* gene was replaced with the *His3* gene was kindly provided by Drs. M. Conrad and J. Conaway. For rescue of the mutant strain, *Arabidopsis AtRbx1* gene was fused to the Gal1 promoter into plasmid pYES2 (Invitrogen). The MCY557 strain was transformed with either the empty pYES2 or the pYES2-AtRbx1 vectors, and Ura^+ transformants were selected. Sporulated diploids were dissected. For the manipulation of these strains, we used the conditions described in Ref. 48.

Yeast Two-hybrid Analysis—The coding region of *AtRbx1;1* was PCR-amplified using oligonucleotide 5′-CGCGGATCCTTAGTGACCATATTTCTGAAACT-3′ and oligonucleotide 5′-CCGGAATTCATGGCGACTCTAGACTCCGACGTTA-3′ as the upstream and downstream primers, respectively, and subsequently cloned into the *Eco*RI and *Bam*HI sites of pGBKT7 vector (Clontech), resulting in plasmid pGBKT7-AtRbx1. The cloning of pGBKT7-RH2b is described in Ref. 49. The coding region of AtCul1 (At4g02570, see Ref. 45) was PCR-amplified using oligonucleotide 5′-TTGTCAACGGATCCATGGAGCGCAAGACTATTGACTTG-3′ and oligonucleotide 5′-GACCACTAGTCCTAAGCCAAGTACCTAAACATG-3′ as the upstream and downstream primers, respectively, and subsequently cloned into *Bam*HI-*Spe*I of pBluescript vector (Stratagene), resulting in plasmid pKS-AtCul1. The vector was digested by *Eco*RI and *Sac*I, and the excised DNA fragment was cloned into pGADT7 vector (Clontech), resulting in plasmid pGADT7-AtCul1. The coding region of AtCul4 (At5g46210, see Ref. 45) was PCR-amplified using oligonucleotide 5′-AGGAATTCATGTCTCTTCCTACCAAACGCTCTA-3′ and oligonucleotide 5′-CGGGATCCCCTAAGCAAGATAATTGTATATCTGA-3′ as the upstream and downstream primers, respectively, and subsequently cloned into *Eco*RI and *Sac*I sites of pGADT7 vector, resulting in plasmid pGADT7-AtCul4. The derived plasmids were sequenced to confirm the absence of errors from PCR amplification and the correct in-frame fusion with the GAL4 DNA binding and activation domains. All the pGBKT7 vectors (either empty or encoding RH2b or AtRbx1) were introduced into the yeast host haploid strain AH109, whereas all the pGADT7 vectors (either empty or encoding AtCul1 or AtCul4) were introduced into the yeast host haploid strain Y187. Y187 strain has a stronger promoter to drive *lacZ* expression than AH109. Interactions between the fusion proteins were assayed in the AH109/Y187 diploid strains according to the recommendations of the manufacturer (Clontech).

RESULTS

Arabidopsis thaliana Genome Encodes Two Proteins Structurally Related to Yeast and Human Rbx1—A. thaliana data base searches led to the identification of two different genes called *AtRbx1;1* and *AtRbx1;2*, located on chromosome 5 (At5g20570) and chromosome 3 (At3g42830), respectively. The sequence of the longest EST for *AtRbx1;1* was determined, and it encodes an 118-amino acid open reading frame, which is complete at its N-terminal end as indicated by an in-frame stop codon upstream of the initiation codon. AtRbx1;1 and the predicted AtRbx1;2 protein sequences exhibit 87% sequence identity. Both proteins are closely related to human Rbx1 protein (86% identity and over 91% similarity between AtRbx1;1 and HsRbx1 sequences). The plant sequences were aligned with yeast and different animal Rbx1 protein sequences (see Fig. 1). All the residues proposed to form the zinc binding sites (50) are perfectly conserved. Interestingly, both *Arabidopsis* proteins belong to the Roc1/Rbx1 subgroup and are more distant from the Roc2/Rbx2 proteins.

AtRbx1 Complements the Lethality of Yeast MCY557 rbx1 Deletion Strain—rbx1 is an essential gene in yeast, and its inactivation arrests the cell cycle at the G_1/S transition and results in the stabilization of different SCF substrates, like Sic1p and Cln2p (12, 14). The diploid *rbx1* deletion strain MCY557 (12), which produces only two viable spores from each tetrad, was transformed with a plasmid expressing either the plant or the human *Rbx1* gene. After tetrad dissection, all four spores were viable on YPD and SD-uracil media, indicating that both plant (Fig. 2) and mammalian (Refs. 12 and 14 and data not shown) *Rbx1* genes were able to rescue the viability defect of the yeast mutant strain.

AtRbx1 Interacts with AtCul1 and AtCul4 in a Yeast Two-hybrid Assay and Is Part of the SCF Complex Containing Both AtCul1 and ASK Proteins—We next determined whether AtRbx1 interacts with plant cullins (Fig. 3). *AtRbx1* was cloned into the pGBKT7 bait plasmid to produce a fusion protein with Gal4 DNA binding domain. Another small *Arabidopsis* RingH2 protein (49) not related to the primary protein sequence of AtRbx1 was also introduced into pGBKT7 plasmid. AtCul1 (At4g02570) and AtCul4 (At5g46210) were cloned into the prey pGADT7 vector to produce fusion proteins with the Gal4 activation domain. Only AtRbx1 and not the other small RingH2 protein interacted with the cullin proteins by the two-hybrid assay (Fig. 3*A*). β-Galactosidase activities, used to quantify the protein interactions, indicated that the AtRbx1 interacts similarly with both AtCul1 and AtCul4 proteins (Fig. 3*B*).

To further demonstrate the physical interaction between AtRbx1 and the AtCul1 protein, we performed pull-down assays. AtRbx1;1 was expressed in *Escherichia coli* as a translational fusion protein with GST. The purified GST-Rbx1 fusion protein (or GST alone as a control) was incubated with *Arabidopsis* crude protein extracts, and the bound plant proteins were immunoblotted with the AtCul1 antibody. AtCul1 co-purified with the GST-Rbx1 fusion protein but not with the GST protein alone (Fig. 3*C*). AtCul1 protein migrated as a doublet, with the weaker upper band corresponding most obviously to the Rub1-modified form of the protein (51). The identity of the cullin protein was further confirmed by the competition assay using the AtCul1 peptide.

In addition, SCF complexes were immunoprecipitated from transgenic plant extracts expressing either the *myc*-tagged ASK1 or the *myc*-tagged ASK2 proteins and analyzed for the presence of AtRbx1 and AtCul1. Both AtRbx1 and AtCul1 proteins co-immunoprecipitated with either *myc*-tagged ASK1

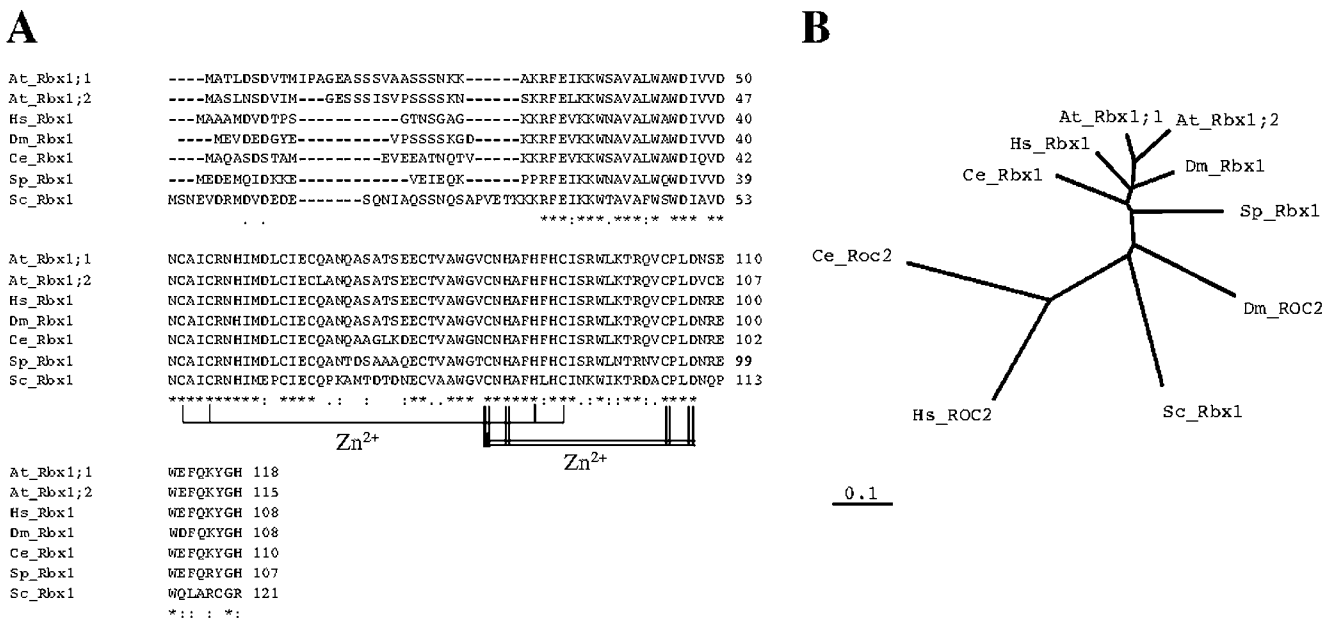

FIG. 1. **Sequence alignments and phylogenetic analysis of the AtRbx1 proteins.** *A*, alignment of the *Arabidopsis* amino acid sequences AtRbx1;1 (accession no. AAL13435) and AtRbx1;2 (CAB87200) with those of human (X73608), *Drosophila* (AAF45536.1), worm (T27823), *Schizosaccharomyces pombe* (T38310), and *Saccharomyces cerevisiae* (YOL133w). Multiple sequence alignment was performed with the ClustalW (1.81) program. *Asterisks* and *dots* indicate identical and conserved amino acids, respectively. The potential zinc coordination of the cysteine and histidine residues is schematically represented. *B*, phylogenetic analysis of the Rbx1/Roc1 protein family (for accession numbers, see *A*) and human (AAD25962.1), *Drosophila* (AAF47382.1), and worm (T29620) Roc2 proteins performed with the Clustal and TreeViewPPC programs. Branch lengths are proportional to phylogenic distances.

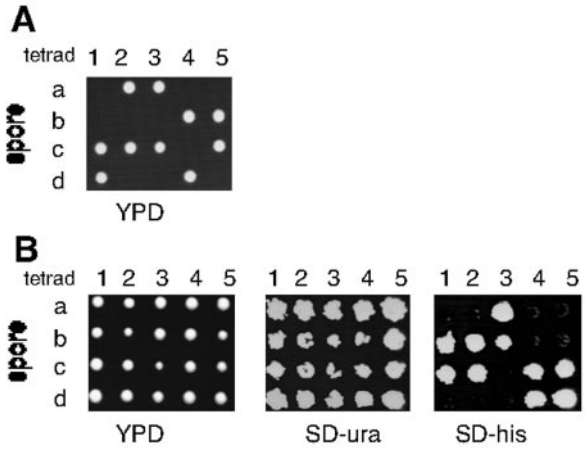

FIG. 2. **Sporulation and tetrad dissection of a heterozygous *RBX1/rbx1*Δ strain containing either the empty pYES2 (*A*) or the pYES2-AtRbx1 (*B*) vectors.** The plate, containing the germinated spores expressing AtRbx1, was replicated onto SD−uracil and SD−histidine. Although *AtRbx1* sequence was put under the control of the Gal1 promoter, the complementation worked already on media containing dextrose instead of galactose, probably because of the leakage of this promoter. The same results were obtained on complete galactose medium (data not shown).

(data not shown) or the *myc*-tagged ASK2 (Fig. 3*D*). It is worth noting that the interaction between AtRbx1 and the ASK proteins is indirect and most likely mediated by the AtCul1 protein. Thus, our data clearly demonstrate the ASK1/2, AtCul1, and AtRbx1 proteins form complexes *in planta*.

Expression of AtRbx1 in Plants and in Response to External Stimuli—Based on the available EST sequences, it appears that *AtRbx1;1* is expressed at a higher level than *AtRbx1;2*; In the current data bases, six different ESTs are found for *AtRbx1;1*, but none for *AtRbx1;2*. To determine whether the *AtRbx1;2* gene is expressed, we performed semiquantitative RT-PCR with specific primers designed from the 3′-untranslated region of both genes. Whereas *AtRbx1;1* primer set efficiently amplified *AtRbx1;1* transcript from floral buds, stems, and roots, no PCR product was obtained with *AtRbx1;2* primer set (data not shown), suggesting that *AtRbx1;2* gene is very poorly or not at all expressed, at least in these plant organs.

RNA blot analyses were performed to investigate *AtRbx1* expression, and its mRNAs could be detected in all the plant organs analyzed (Fig. 4*A*). Nevertheless its mRNAs accumulate, as histone H4, at higher levels in flowers and germinated seeds, indicating a higher expression in tissues containing actively dividing cells. This was reinforced by the finding that its expression is also stimulated during re-initiation of mitotic activity in *Arabidopsis* (Fig. 4*B*). In this system, differentiated leaf cells are stimulated to re-enter the cell cycle by wounding and auxin stimulation (42). In contrast to histone H4, which is expressed at the highest level at 48 h when most of the cells are in S phase (48 h of culture corresponding to the highest [^{3}H]dTTP incorporation, data not shown), *AtRbx1* mRNAs accumulate at different times during the culture. Thus, we have no evidence for a specific cell cycle phase accumulation of *AtRbx1* transcripts.

Because SCF-dependent proteolysis was shown to play a key function in auxin signaling (reviewed in Refs. 52 and 53), we investigated whether *AtRbx1* gene transcription can itself be induced by auxin. We chose an experimental system using hypocotyls of etiolated seedling because of its rapid response to auxin (41). The level of *AtRbx1* transcript remained unchanged 1 h after the treatment with auxins, whereas the positive control *SAUR* gene responded positively to the treatments (Fig. 4*C*). It is thus unlikely that *AtRbx1* belongs to the auxin-responsive gene family. We also tested *AtRbx1* gene expression under different growth conditions including dark to light transition and heat shock. Whereas *AtRbx1* gene did not respond to light (Fig. 4*D*), its mRNAs rapidly decayed 1 h after heat shock treatment (Fig. 4*E*).

Modulation of AtRbx1 Protein Level in Arabidopsis—To investigate the function of *AtRbx1 in planta*, we designed con-

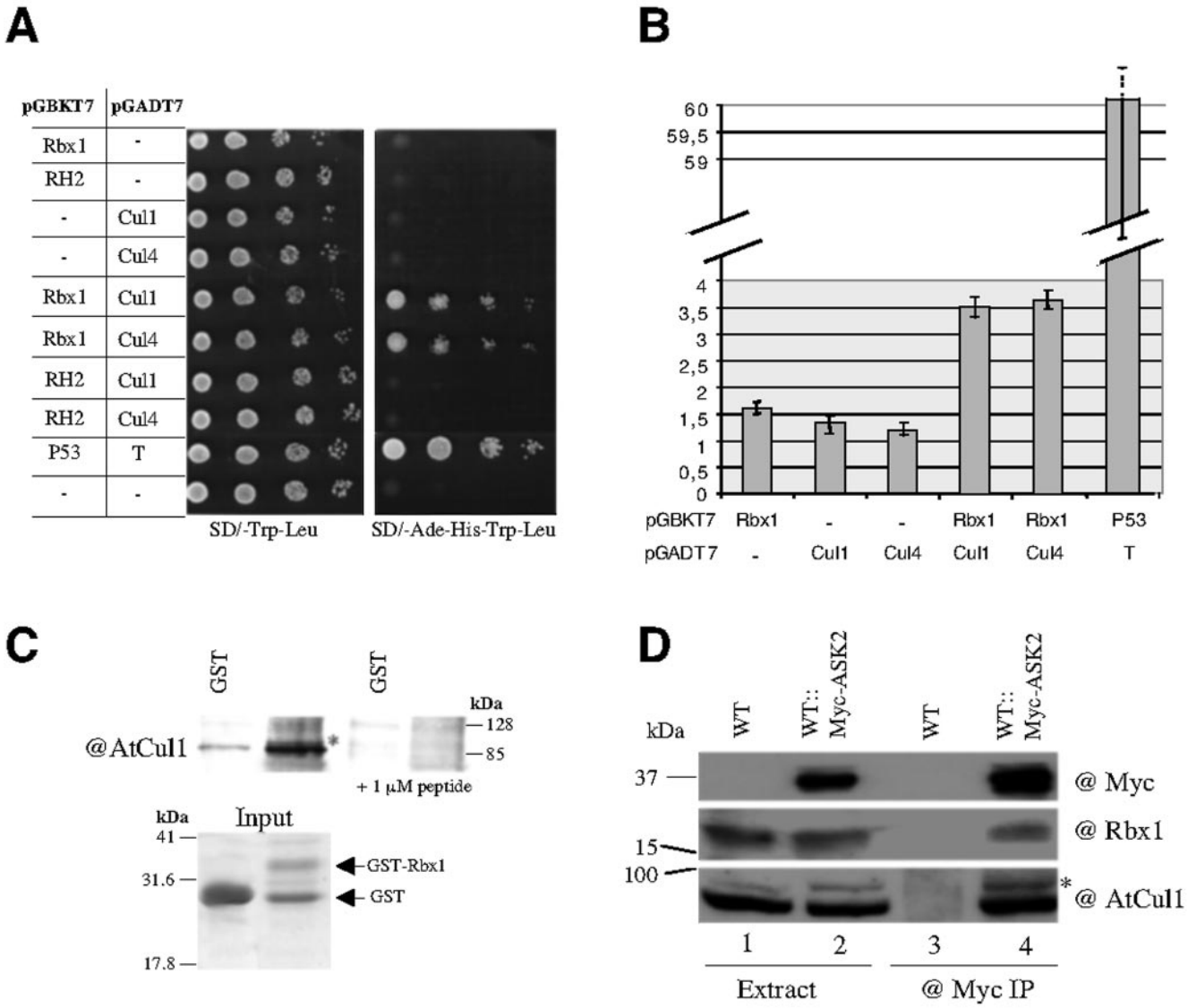

FIG. 3. **AtRbx1;1 protein interacts with *Arabidopsis* cullin and SKP1-related proteins.** *A*, yeast diploid AH109/Y187 cells co-expressing the indicated proteins were plated onto media lacking tryptophan and leucine (SD/−Trp−Leu) to check for the presence of both bait and prey plasmids or onto media lacking adenine, histidine, tryptophan, and leucine (SD/−Ade−His−Trp−Leu) to assay for the interaction between bait and prey proteins. *B*, yeast diploid AH109/Y187 cells co-expressing the indicated proteins were tested for the β-galactosidase activities. As a control we used pGBKT7–53 and pGADT7-T control vectors (Clontech), which give strong protein interaction. The galactosidase activity is given as the mean ± S.D. of five independent yeast lines for each combination of constructs. *C*, pull-down assays with either GST or Rbx1-GST were probed with the specific *Arabidopsis* anti-Cullin1 antibody (*@AtCul1*). The *asterisk* indicates the Rub1-modified form of AtCul1. The competition experiment was performed with 1 μM antigen peptide (shown on the *right side* of the panel). *D*, co-immunoprecipitation assay. Protein extracts from wild type (*WT*) (*lane 1*) and transgenic plants expressing the *myc*-tagged ASK2 (*WT*::*myc-ASK2*, *lane 2*) were immunoprecipitated with anti-*myc* antibody (*lanes 3* and *4*). The resulting immunoprecipitate (*IP*) was resolved on SDS-PAGE and detected with the indicated antibodies. The *asterisk* indicates the Rub1-modified form of AtCul1.

structs to either overexpress or silence the gene in *Arabidopsis* (see Fig. 5). Because *Rbx1* is an essential gene in budding yeast and is involved in SCF-dependent ubiquitylation and degradation of cell cycle regulatory proteins (12, 14, 15), we investigated its function in plants by setting up inducible PTGS and overexpression assays. We also engineered different control plants: either empty vector transgenic plants or plants expressing GFP or GUS under the control of the inducible vector. GFP and GUS expression were confirmed in some of the plants. Seeds of the T1 generation from more than 25 different transgenic lines for each construct were sown *in vitro* in the presence or absence of Dex (1 μM) and were analyzed phenotypically and at the molecular level.

Accordingly to the results published in Ref. 54, but to a much lesser extent, 2 control lines (pTA::4 and pTA::GFP6) of 39 lines analyzed (24 empty vector, 10 pTA::GUS, and 5 pTA::GFP lines), showed alteration in seedling development. Line pTA::GFP6 had a low yield of germination, whereas line pTA::4 showed shrink-shaped cotyledons (see below).

As expected higher levels of *AtRbx1* mRNA and protein were found in the pTA::Rbx1-overexpressing lines (called sense lines) (Fig. 6 (*A* and *B*) and data not shown). The antibody used was specific, as demonstrated by the competition assays (Fig. 6*C*). 19 out of 27 sense lines analyzed showed a shrink cotyledon shape (Fig. 7, *A* and *B*). However, a similar phenotype was found in control line pTA::4 (data not shown), exhibiting strong expression of the chimeric GVG transcription factor (38) and the induction of the defensin gene PDF1.2 (55) (Fig. 6*A*). Thus we did not consider the shrinkage of the cotyledons as a phenotype because of Rbx1 overexpression, but rather as side effects of the vector. Furthermore in all sense lines and control lines, the development of the leaves was not disturbed and

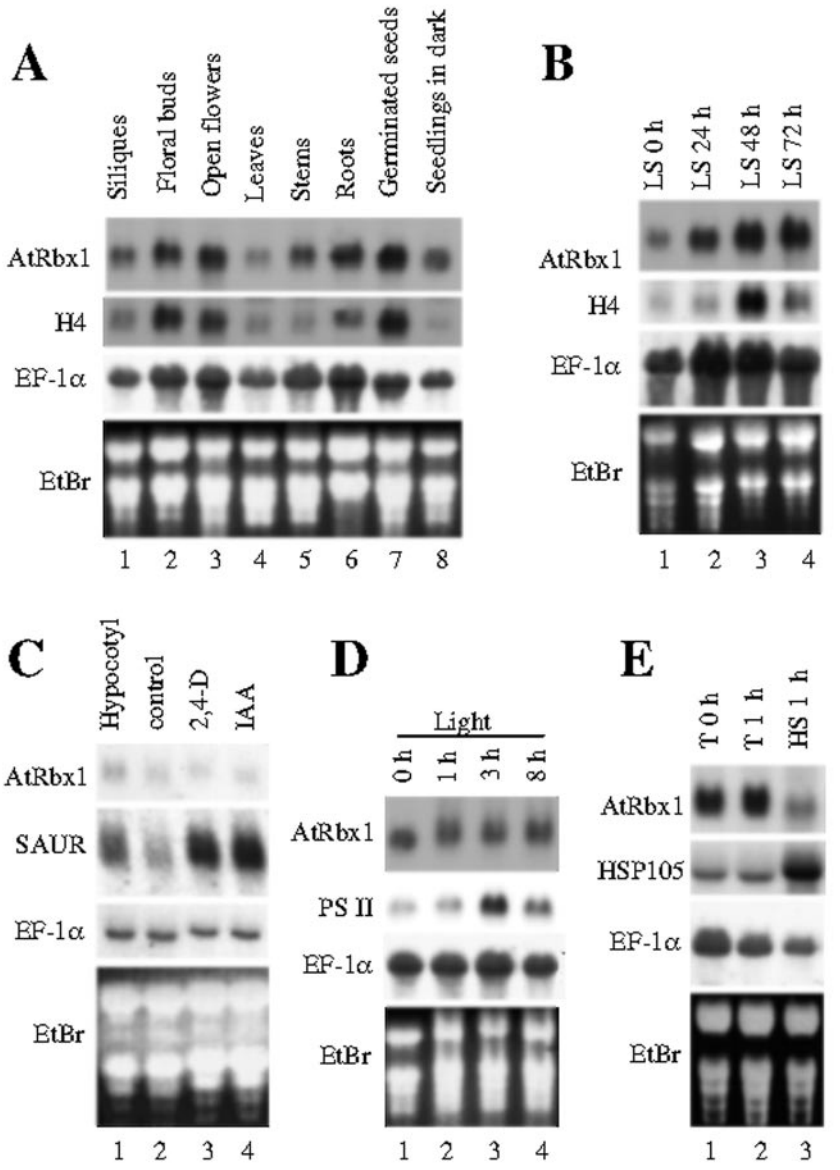

FIG. 4. ***AtRbx1* mRNA accumulation in various *Arabidopsis* organs, during re-initiation of mitotic activity in leaf strip cultures and after hormones, light, and heat shock treatments.** *A*, total RNA was extracted from silique (*lane 1*), floral buds (*lane 2*), open flowers (*lane 3*), leaves (*lane 4*), stems (*lane 5*), roots (*lane 6*), 3-day-old germinating seeds (*lane 7*), and seedlings germinated in the dark (*lane 8*). *B*, total RNA was extracted from leaf strips (*LS*) incubated in a medium suitable for cell division for 0 h (*lane 1*), 24 h (*lane 2*), 48 h (*lane 3*), and 72 h (*lane 4*). *C*, effects of auxins. *Arabidopsis* hypocotyl sections were incubated in the absence (control) or in the presence of 11 mg/liter 2,4-dichlorophenoxyacetic acid or 1,8 mg/liter IAA for 1 h, and then used for total RNA preparation. *D*, effects of dark to light transition. 12-day-old *Arabidopsis* seedlings grown in the dark were transferred into light, and total RNA was extracted at various times as indicated. *E*, 14-day-old *Arabidopsis* seedlings were subjected to a heat shock at 38 °C during 90 min and than allowed to recover during 1 h at 22 °C before being collected. Blots were hybridized with the indicated random-primed ^{32}P-labeled probes.

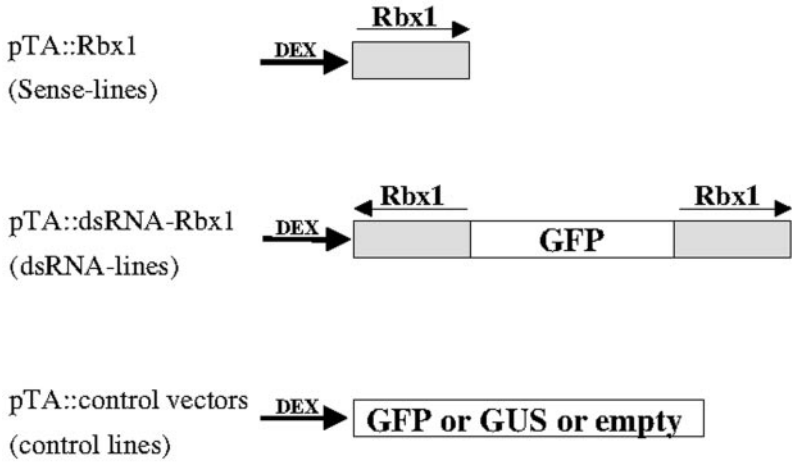

FIG. 5. **Schematic representation of the vectors used for plant transformation.** *Gray bars* represent AtRbx1;1 sequence, and its orientation is indicated by *arrow lines*.

plants grew normally on the Dex-containing medium, at least during the early vegetative growth phase.

Similar to the sense lines, most of the pTA::dsRNA lines (called dsRNA lines) (21/28 lines, 75%) also showed the shrink-shaped cotyledon phenotype (data not shown). *AtRbx1* mRNA and protein levels were found reduced in those lines (Fig. 8*A*, *lanes 3* and *4*). Interestingly, 83% of the dsRNA lines grown for more than 30 days in the presence of Dex developed small green bushy plants (5–30%/plate), as illustrated for line dsRNA-84 (Fig. 7*C*) with reduced AtRbx1 RNA and protein

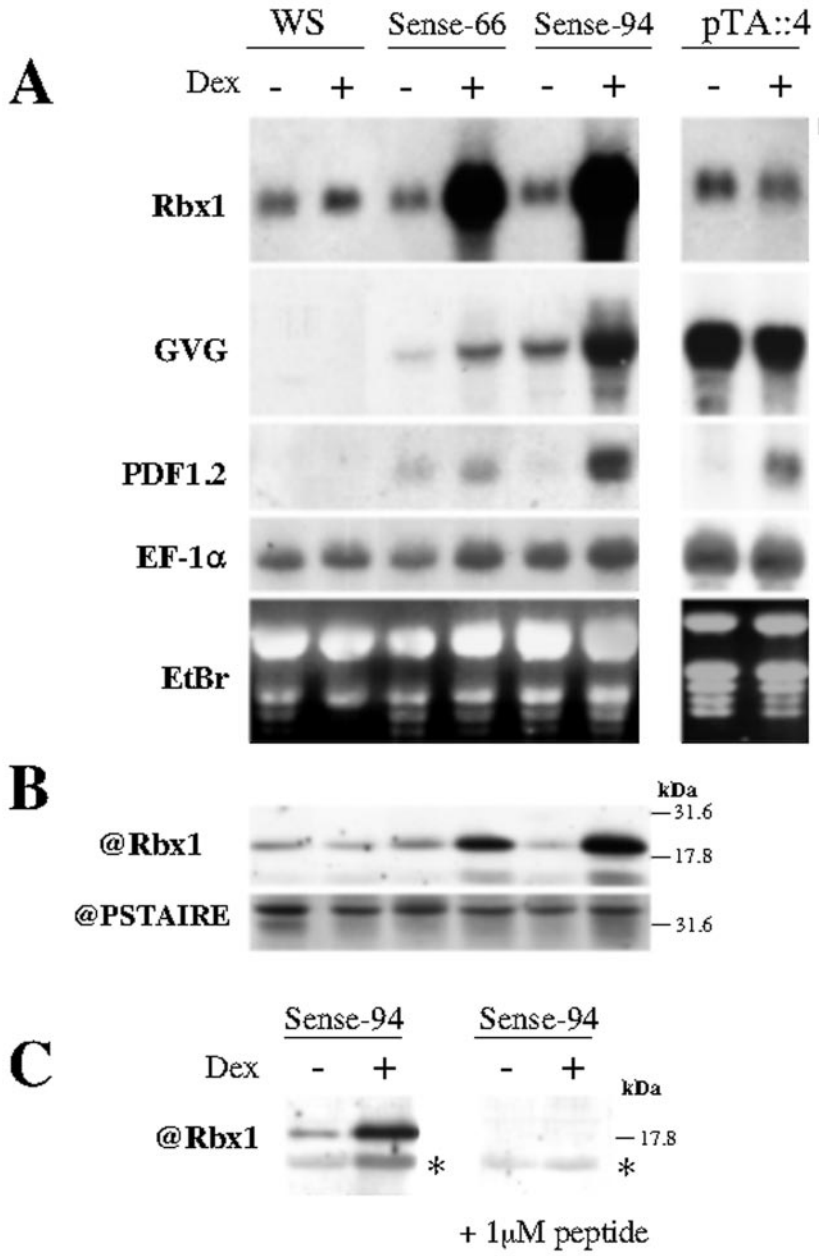

FIG. 6. **Northern and Western blot analysis of *AtRbx1*-overexpressing and control lines.** The identity of the lines is indicated: WS (non-transformed *Arabidopsis* Wassilewskija ecotype), *AtRbx1*-overexpressing lines Sense-66 and Sense-94, and control line pTA::4. *A*, total RNA was isolated from 10-day-old *Arabidopsis* seedlings germinated in presence or absence of Dex as indicated. The RNA gel blot analysis was performed by successive hybridization with different probes, as indicated. *B*, total proteins were prepared from the same samples as indicated in *A*. Western blots were performed with the antibodies against AtRbx1 (*@AtRbx1*) and the conserved CDK kinase motif PSTAIRE (*@PSTAIRE*). *C*, competition experiment realized with 1 μM AtRbx1;1 peptide (*right panel*) or without peptide (*left panel*) on the same extracts from line Sense-94, as indicated in *B*. The *asterisk* indicates a nonspecific cross-reacting protein band.

levels (Fig. 8*A*, *lane 5*). When the 3-week-old *in vitro* bushy plants were transferred to soil, either they remained dwarf but produced few flowers (Fig. 7*D*, *inset*) or they developed plants with reduced apical dominance (data not shown). Because SCF pathway is involved in auxin signaling (reviewed in Ref. 53), we expected to find auxin-related phenotypes. Indeed, ~10% of the T0 dsRNA lines already showed reduced apical dominance, probably as a result of the leaky expression of the promoter. Similarly, plants exhibiting a reduction in apical dominance with a strong increase in the number of lateral branches were observed in the progeny of several dsRNA lines, and those plants always exhibited a reduction of *AtRbx1* mRNA levels (as illustrated for line dsRNA-76; Fig. 7, *E* and *inset*). A more detailed analysis of auxin responses in these lines is under way.

Interestingly, in three dsRNA lines (dsRNA-2, dsRNA-20, and dsRNA-33), the development of the seedlings was severely impaired (as shown for line dsRNA-2; Fig. 7, *F* and *G*). In those plants, and in contrast to the control or non-induced lines, cotyledons did not develop at all (remaining white) and strong leaf growth retardation and leaf expansion effects were observed. At 10 days after germination, the average length of cotyledons for the dsRNA-2 transgenic plants was 0.82 mm ($\pm$ 0.05 mm, $n = 20$) compared with 2.48 mm ($\pm$ 0.12 mm, $n = 23$) for cotyledons of Dex-treated wild type plants. At this stage, no difference could be found in cotyledon vascularization patterns (data not shown), overall tissue organization, or cellular size (Fig. 7, *H* and *I*). Only the plastid content was found to be different, exhibiting swollen plastids phenotypically identical to amyloplasts. High starch content of the latter was confirmed by Lugol staining (data not shown). Nevertheless at a latter stage (3 weeks after germination), both the size and shape of cotyledon epidermal cells were different. Whereas in the non-induced dsRNA-2 line the average area of cotyledon epidermal cells was 8259 μm^2 ($\pm$ 3948 μm^2, $n = 115$), this value was reduced by a factor of 10 in the AtRbx1-silenced plants (average area of the cells was 801 μm^2 ($\pm$ 338 μm^2, $n = 115$)).

AtRbx1 mRNA (Fig. 8*B*, *lane 3*) and protein (Fig. 9) levels were strongly reduced in those lines, but still detectable. We believe that the strong developmental alteration found in those

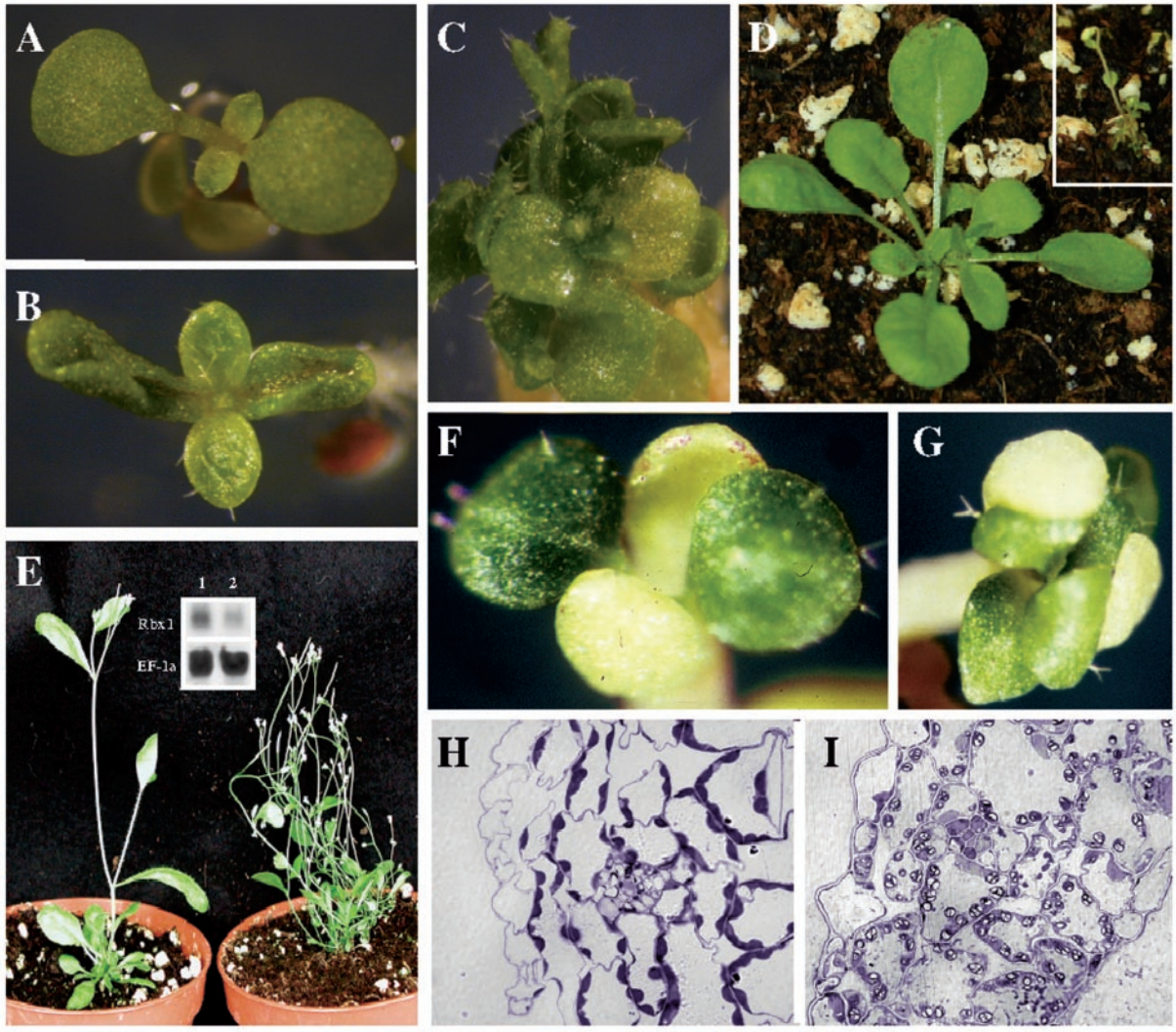

FIG. 7. **Representative plant phenotypes from sense and dsRNA transgenic lines.** *A* and *B*, 10-day-old transgenic plant (overexpressor line Sense-94) grown onto MS medium (*A*) or medium containing 1 μM Dex (*B*). *C*, 3-week-old *in vitro* grown bushy plant (line dsRNA-84). *D*, *inset*, 3-week-old dsRNA transgenic plant (line dsRNA-71) grown first *in vitro* in presence of Dex and than transferred to soil and let to grow for 2 more weeks. As a control, a plant of the same line, but grown first *in vitro* without Dex before transfer to soil, was used. Photographs were taken at the same magnification. *E*, 4-week-old wild type (*left*) and dsRNA transgenic plants (line dsRNA-76) (*right*) grown on soil without Dex. The dsRNA line exhibited a reduction in apical dominance, and this was correlated with a reduction of the *AtRbx1* mRNA level (see *inset*). *F* and *G*, dsRNA transgenic plant (line dsRNA-2) with poorly developed cotyledons and leaves. Pictures were taken at 12 days (*F*) and 22 days (*G*) after germination. *H* and *I*, toluidine blue-stained thin sections of 8-day-old plants showing normal shaped chloroplasts in green wild type cotyledon (*H*), compared with round and swollen amyloplasts in white cotyledon (dsRNA-2 line) (*I*).

dsRNA lines is caused by the Rbx1 depletion and not by the chimeric GVG transcription factor expression (or other effects) because this phenotype was never found in control or Rbx1-overexpressing lines. It is also worth noting that the intermediary RNA can be detected by both AtRbx1 and GFP probes and that at least some of the spacer-GFP RNA always accumulates in the Dex-induced plants (Fig. 8*B*). More than 30 plants of line dsRNA-2 (at the stage indicated in Fig. 7*F*) were transferred to plates with or without Dex. One week later, only the plants on the Dex-free medium recovered, developing normal leaves and re-accumulating the *AtRbx1* transcripts (see Fig. 8*B*, *lane 4*). Nevertheless, some of the plants became bushy (data not shown). Thus, in contrast to a systemic PTGS reaction (reviewed in Refs. 56 and 57), silencing occurring in the dsRNA lines was reversible.

To confirm that *AtRbx1* mRNA decay was the result of dsRNA-induced PTGS, we assayed for the presence of 21–23-nucleotide *AtRbx1* fragments in the Dex-treated plants. Six-week-old rosette plants of dsRNA-2 line, as well as pTA::GFP control and wild type plants, grown under standard conditions in the green house were sprayed with a solution of 10 μM Dex and harvested at different times. Semiquantitative RT-PCR analysis of the plants indicated a strong reduction of *AtRbx1* mRNAs 4 days after Dex treatment, specifically in the dsRNA line (Fig. 8*C*). 21–23-nucleotide species were readily detected in the low molecular weight RNA fractions of the Dex-treated pTA::dsRNA plants (Fig. 8*D*), but not in the GFP-expressing control lines or wild type plants (data not shown). The small RNA fragments appeared 24 h after the treatment and reached the highest accumulation at 96 h.

To understand the biochemical basis of the severe growth defects observed in some of the dsRNA lines, protein extracts from dsRNA-2 line and control line were blotted with different antibodies (Fig. 9). Interestingly, we noted that AtRbx1-depleted seedlings do not only show a strong reduction of AtRbx1 protein level, but also a decreased AtCul1 protein level. In fact, both Rub1-modified and unmodified AtCul1 protein bands were weaker. To check whether the reductions of AtRbx1 and, to a lesser extent, AtCul1 would affect the pattern of ubiquitin conjugates, the blot was probed with an anti-ubiquitin antibody

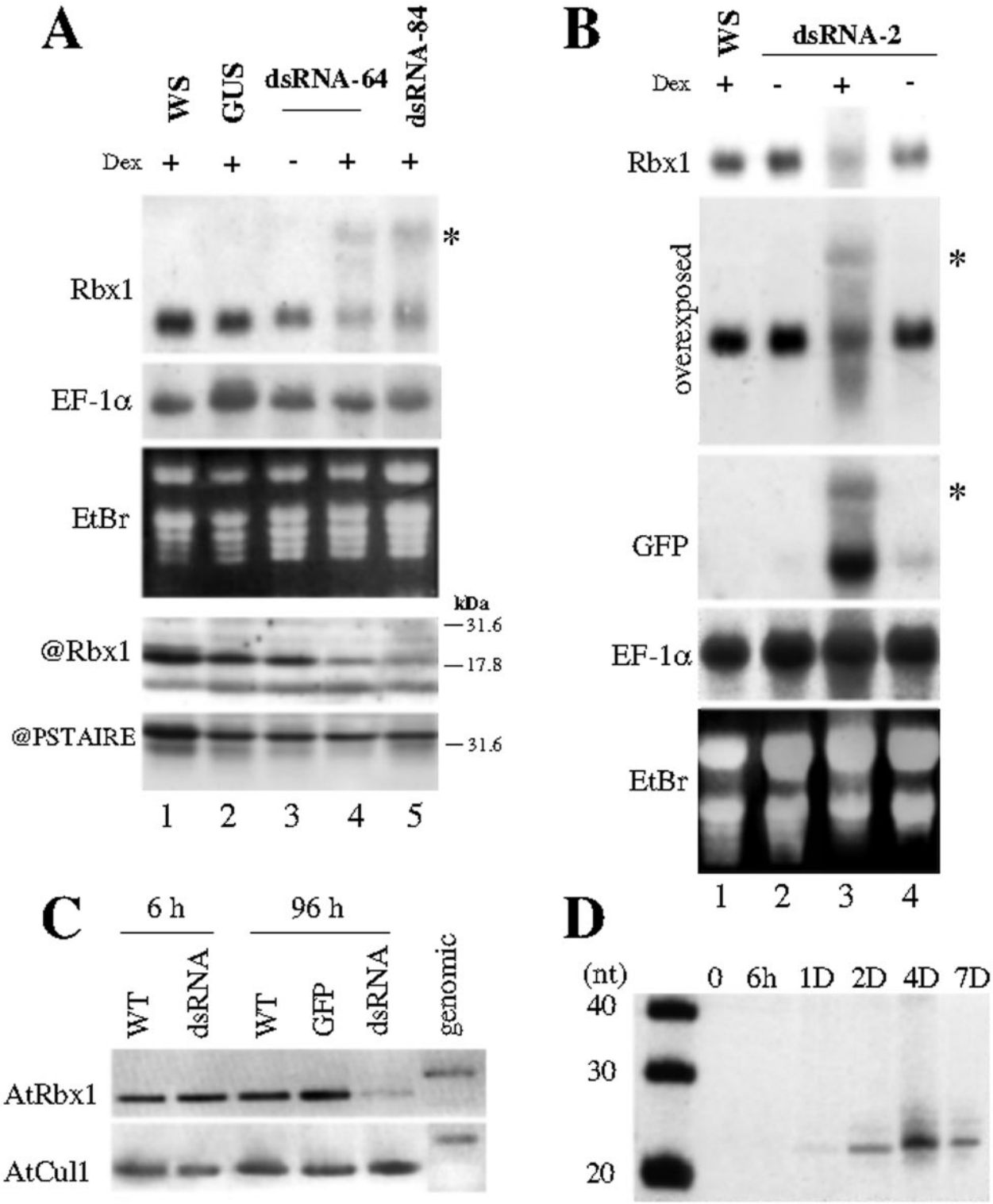

FIG. 8. **Molecular analysis of *AtRbx1* dsRNA and control lines.** The identity of the lines is indicated: WS (non-transformed *Arabidopsis* Wassilewskija ecotype), GUS (pTA-GUS-transformed *Arabidopsis* line), and dsRNA lines 2, 64 and 84. *A*, AtRbx1 mRNA and protein accumulation in dsRNA and control lines. Total RNA was isolated from 10-day-old *Arabidopsis* control seedlings (*lanes 1* and *2*) or from line dsRNA-64 (*lanes 3* and *4*) germinated in the absence or presence of Dex. *Lane 5* corresponds to the *in vitro* bushy plants produced after longer periods of growth on Dex medium (here line dsRNA-84, shown on Fig. 7*C*). The *asterisk* indicates the intermediary RNA. Western blots were performed with the antibodies against AtRbx1 (@*AtRbx1*) and the conserved CDK kinase motif PSTAIRE (@*PSTAIRE*). *B*, induction and reversion of PTGS in the dsRNA lines. Total RNA was isolated from 10-day-old *Arabidopsis* seedlings germinated in absence or presence of Dex (*lanes 2* and *3*, respectively). Total RNA was also isolated from transgenic seedlings first grown on Dex medium for 12 days, then transferred to a Dex-free medium for 7 days (*lane 4*). The RNA gel blot analysis was performed by successive hybridization with different probes, as indicated. *Asterisks* indicate the intermediary RNA. *C*, RT-PCR analysis of dsRNA (line dsRNA-2) and control lines after spraying with a solution of 10 μM Dex and harvested at different times after the treatment. For controls, RT-PCR reactions were performed with an oligonucleotide set for *AtCul1*. *D*, Northern hybridization analysis of equal amounts of low molecular weight RNA from the Dex-sprayed dsRNA plants (dsRNA-2), at different times after the treatment. The blot was hybridized with AtRbx1 *in vitro*-transcribed ^{32}P-labeled RNA probe. The *lane* on the *left* contains 5′-^{32}P-labeled oligomers as size markers.

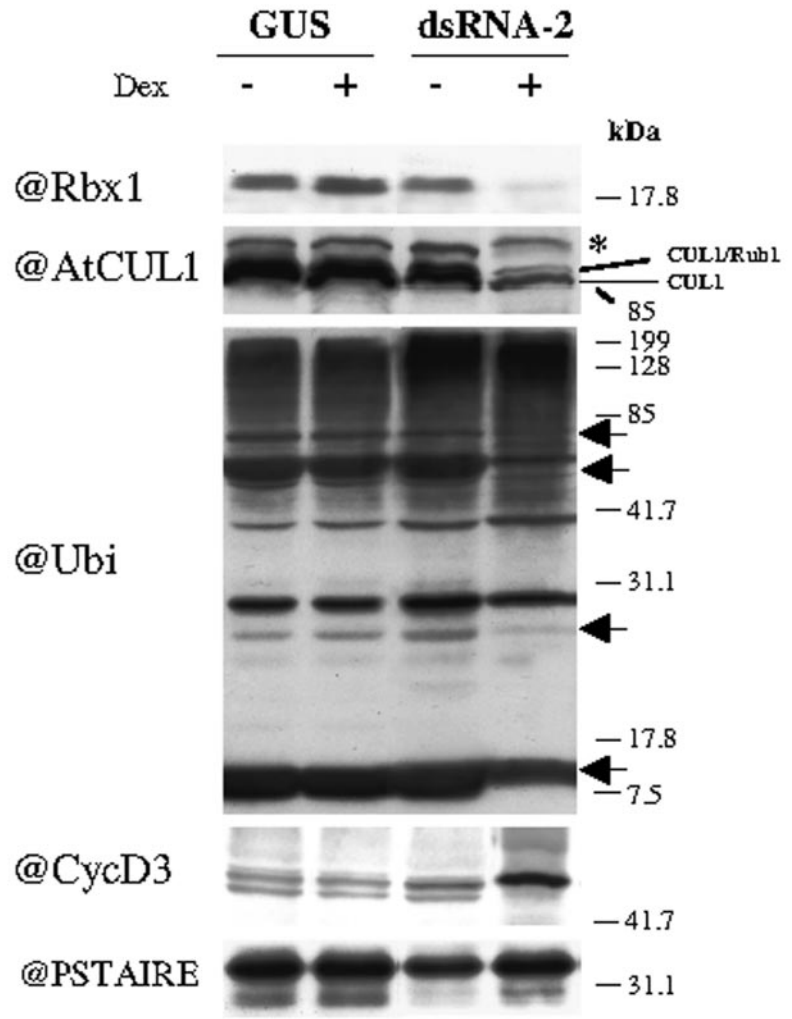

FIG. 9. **Western blot analysis of *AtRbx1* dsRNA and control lines.** The identity of the lines is indicated: GUS (pTA-GUS-transformed *Arabidopsis* line) and dsRNA-2 lines. Total proteins were prepared from 10-days old *Arabidopsis* seedlings germinated in presence or absence of Dex as indicated. Western blots were performed with the antibodies against AtRbx1 (@*AtRbx1*), AtCul1 (@*AtCUL1*), ubiquitin-protein conjugates (@*Ubi*), cyclin D3 (@*CycD3*), and the conserved CDK kinase motif PSTAIRE (@*PSTAIRE*). The *asterisk* indicates a nonspecific cross-reacting protein band, whereas the *arrows* indicate several protein bands that disappeared or were reduced in the Dex-induced dsRNA line.

that recognizes both free and conjugated ubiquitin. Indeed, we noted that several protein bands either disappeared or were strongly reduced in the Dex-induced dsRNA line. The level of free ubiquitin also was reduced in those plants. However, the pattern of most ubiquitin conjugates were still similar between the non-induced and the induced line. This may not be surprising because *Arabidopsis* counts many other E3s aside the SCF (58).

Mammalian D-type cyclins are highly unstable proteins, and several experiments substantiate the involvement of SCF complexes in their degradation (59, 60). Similarly to the animal D-type cyclins, the expression of *Arabidopsis* cyclin D3 was found regulated by growth signals and the protein shown to be very unstable (47, 61, 62). Interestingly, in the Rbx1-depleted plants, we found a significant higher level of cyclin D3 protein (Fig. 9) whereas cyclin D3 mRNAs accumulated at a similar level than in the Dex non-induced or control plants (data not shown). However, this protein band is detected at ~46 kDa, whereas cyclin D3 detected in roots is ~55 kDa (47). Because the antibody was raised against the C-terminal peptide of cyclin D3 (47), the 46-kDa form of the protein must represent the loss of an N-terminal fragment or could be an alternative splice form or a modified form of the protein. Whether cyclin D3 is a target of plant SCF complexes remains to be demonstrated.

DISCUSSION

SCF is a highly conserved ubiquitin protein ligase that is constituted by at least four subunits: SKP1 (called ASK1 in *Arabidopsis*), Cul1, F-box proteins, and the Ring-H2 finger protein Rbx1 (reviewed in Ref. 16). In plants the functions of the SCF have been highlighted by the characterization of different loss-of-function mutants in genes encoding F-box proteins (see Introduction). The F-box protein is the specific adapter interacting directly with the substrate(s) and allowing its ubiquitylation. The best understood SCF complex in plants is probably SCF^{Tir1}, in which the F-box protein Tir1 interacts with a subdomain of the AUX/IAA protein, leading to their degradation after auxin stimulation (see Ref. 26 and references therein). In addition to the F-box proteins, *Arabidopsis* genome sequence also revealed the presence of SKP1- and cullin-related genes. Whereas there is only a single SKP1 protein identified so far in humans, there are 19 SKP1 orthologs present in *Arabidopsis* genome (34). The function of only one of the plant *SKP1*-related gene, called *ASK1*, has been investigated so far. Mutation of the *ASK1* gene produces diverse phenotypes including abnormal floral morphology (63), male sterility (64), and auxin resistance (21, 65). Nevertheless, the homozygous mutant is still viable, suggesting some functional redundancy with other *SKP1*-related genes. Cullins also belong to a multigenic gene family, and, in *Arabidopsis,* there are 11 cullin-related genes. Recently, we investigated the function of one of these genes, *AtCul1*, which is closely related to yeast *CDC53* and human *Cul1* and *Cul2* (45). The homozygous mutant displayed an early arrest in embryogenesis (at the first cell divisions after fertilization of the zygote), indicating that the gene and, as a consequence, SCF-dependent proteolysis are essential in *Arabidopsis*.

In the present work, we characterized in *Arabidopsis* the fourth component of the SCF complex: the Ring-H2 finger protein AtRbx1. *Arabidopsis* encodes two *Rbx1*-related genes: *AtRbx1;1* and *AtRbx1;2*. Accordingly to the essential function of SCF-dependent ubiquitylation in all eukaryotes, *AtRbx1.1* was found expressed in all plant organs. *AtRbx1;2* may only be expressed in particular cell types or at a very low level or even not at all. Interestingly, higher *AtRbx1* mRNA accumulation was found in tissues containing actively dividing cells, suggesting that, as in yeast and animal cells (reviewed in Ref. 2), SCF-dependent ubiquitylation in plants may also be involved in the turnover of key cell cycle regulatory proteins. Interestingly most of *AtRbx1* transcripts (as well as AtCul1 transcripts; data not shown) disappeared after heat shock, suggesting that SCF-dependent ubiquitylation may not play a major role in the proteolytic events following heat stress in plants.

Both our genetic and biochemical data identified *AtRbx1* as the plant ortholog of *Hrt1*/*Rbx1*/*Roc1* in yeast and animal cells. The *Arabidopsis* gene was able to rescue the viability defect of the yeast *Rbx1*-deletion mutant strain. Furthermore, we demonstrated that AtRbx1 protein physically interacted with AtCul1 and is part of a plant SCF complex. Analysis of our dsRNA lines also supported the notion that AtRbx1 is part of plant SCF complexes. Many plants from the dsRNA lines exhibited reduced apical dominance, suggesting reduced auxin response. While our manuscript was under revision, Gray *et al.* (66) reported that, if driven by a constitutive promoter, transgenic *Arabidopsis* plants overexpressing AtRbx1 exhibited reduced auxin response and stabilization of the AXR2/IAA7 protein. In those plants, almost all AtCul1 protein was found modified by Rub1. In contrast, our Dex-induced Sense lines did not show auxin-related phenotypes and examination of AtCul1 protein did not reveal Rub1-hypermodification (data not shown). The reasons of these discrepancies are not clear, but it is possible that the overexpression of AtRbx1 in the Dex-treated plants was not maintained long enough to reveal those phenotypes. In addition, reduction of *AtRbx1* expression in our dsRNA lines led also to a decreased jasmonate response (67). Thus, deregulation of AtRbx1 protein level leads to phenotypes similar to those observed in the *axr1* (68), *tir1* (21), and *coi1* (22) mutants and substantiates the role of AtRbx1 as a component the SCF^{Tir1} and SCF^{Coi1} complexes. Indeed, AtRbx1 coimmunoprecipitated with Coi1 (67) and a GST-AtRbx1 recombinant protein was able to pull down the Tir1 protein (66).

Nevertheless, depending on transgenic lines, more severe phenotypes were observed. Thus, in at least three independent dsRNA lines, seedling development was totally blocked. Consistent with plant survival of those lines, we never found a complete suppression of the *AtRbx1* mRNA and protein. Introduction of an antisense AtRbx1 construct into *Arabidopsis* plants also resulted in the death of young seedlings or caused severe dwarf phenotypes (66). Interestingly, in our dsRNA lines we observed a significant reduction of AtCul1 protein level, suggesting that AtRbx1 protein is necessary to accumulate a stable SCF complex. Thus, SCF-dependent ubiquitylation, not only is essential for *Arabidopsis* embryogenesis (45), but also seems to be required for post-embryonic development (Ref. 66 and this work). The reasons for the developmental arrest in the AtRbx1-depleted seedlings are unknown, but the stabilization of key cell cycle regulatory proteins may be the cause of this arrest. In fungi and animal cells, many cell cycle proteins, particularly at the G_1 to S transition, are subjected to SCF-dependent ubiquitylation (reviewed in Refs. 2, 16, and 69). Among them are the G_1-type cyclins, cyclin E, cyclin-dependent kinase inhibitors, and the E2F-1 transcription factor. Although many of these proteins are conserved in plants (reviewed in Ref. 70), how they are regulated at a post-transcriptional level is poorly understood. Interestingly, in the AtRbx1-silenced plants, we found a higher accumulation of cyclin D3, which like animal D-type cyclins is an unstable protein (47). Whether cyclin D3 is a substrate of a plant SCF complex remains to be demonstrated. Nevertheless, based on the huge number of F-box proteins in *Arabidopsis* (34), it is expected many regulatory proteins are stabilized in the dsRNA-arrested seedlings.

However, the phenotypes observed in the dsRNA transgenic plants may not only arise from functional alteration of Cul1/SCF complexes. In animal cells, it was shown that Rbx1 protein interacts with several other members of the cullin family (13). Accordingly, the essential residues found in the C-terminal globular α/β domain of the Cul1 protein, which are involved in interaction with Rbx1, are also conserved in the other cullin members (17). The function of Cul1-related proteins is only poorly understood, and it is not known whether all of them are part of SCF-like complexes. Cul2 has been shown to assemble a ubiquitin protein-ligase complex, including Rbx1, elongin C, and the SOCS-box family protein VHL (reviewed in Ref. 71). In the yeast two-hybrid assay, we found that AtRbx1 is also able to interact with at least another member of the cullin family, AtCul4, which is functionally distinct from AtCul1 (45). Thus, more experiments will be required to elucidate the function of Rbx1-containing SCF complexes and to understand how they eventually participate in ubiquitin-dependent proteolysis.

Acknowledgments—We thank N.-H. Chua for the inducible vector pTA7002, M. Conrad and J. Conaway for the budding yeast strain MCY557, the Arabidopsis Biological Resource Center and the Kazusa DNA Research Institute (Japan) for providing the translation elongation factor 1-α and photosystem II W clones, D. Inzé for providing the HSP105 clone, B. Winsor for help with the yeast work, Q. Yun for help in plasmid construction, and P. Hammann for DNA sequencing.

REFERENCES

1. Patton, E., Willems, A., and Tyers, M. (1998) *Trends Genet.* **14,** 236–243
2. Deshaies, R. J. (1999) *Annu. Rev. Cell Dev. Biol.* **15,** 435–467
3. Kipreos, E. T., and Pagano, M. (2000) *Genome Biol.* **1,** 3002
4. Bai, C., Sen, P., Hofmann, K., Ma, L., Goebl, M., Harper, J. W., and Elledge, S. J. (1996) *Cell* **86,** 263–274
5. Marti, A., Wirbelauer, C., Scheffner, M., and Krek, W. (1999) *Nat. Cell Biol.* **1,** 14–19
6. Carrano, A. C., Eytan, E., Hershko, A., and Pagano, M. (1999) *Nat. Cell Biol.* **1,** 193–199
7. Strohmaier, H., Spruck, C. H., Kaiser, P., Won, K. A., Sangfelt, O., and Reed, S. I. (2001) *Nature* **413,** 316–322
8. Koepp, D. M., Schaefer, L. K., Ye, X., Keyomarsi, K., Chu, C., Harper, J. W., and Elledge, S. J. (2001) *Science* **294,** 173–177
9. Moberg, K. H., Bell, D. W., Wahrer, D. C., Haber, D. A., and Hariharan, I. K. (2001) *Nature* **413,** 311–316
10. Maniatis, T. (1999) *Genes Dev.* **13,** 505–510
11. Spiegelman, V. S., Slaga, T. J., Pagano, M., Minamoto, T., Ronai, Z., and Fuchs, S. Y. (2000) *Mol. Cell* **5,** 877–882
12. Kamura, T., Koepp, D. M., Conrad, M. N., Skowyra, D., Moreland, R. J., Iliopoulos, O., Lane, W. S., Kaelin, W. G., Jr., Elledge, S. J., Conaway, R. C., Harper, J. W., and Conaway, J. W. (1999) *Science* **284,** 657–661
13. Ohta, T., Michel, J. J., Schottelius, A. J., and Xiong, Y. (1999) *Mol. Cell* **3,** 535–541
14. Seol, J. H., Feldman, R. M., Zachariae, W., Shevchenko, A., Correll, C. C., Lyapina, S., Chi, Y., Galova, M., Claypool, J., Sandmeyer, S., Nasmyth, K., Shevchenko, A., and Deshaies, R. J. (1999) *Genes Dev.* **13,** 1614–1626
15. Skowyra, D., Koepp, D. M., Kamura, T., Conrad, M. N., Conaway, R. C., Conaway, J. W., Elledge, S. J., and Harper, J. W. (1999) *Science* **284,** 662–665
16. Tyers, M., and Jorgensen, P. (2000) *Curr. Opin. Genet. Dev.* **10,** 54–64
17. Zheng, N., Schulman, B. A., Song, L., Miller, J. J., Jeffrey, P. D., Wang, P., Chu, C., Koepp, D. M., Elledge, S. J., Pagano, M., Conaway, R. C., Conaway, J. W., Harper, J. W., and Pavletich, N. P. (2002) *Nature* **416,** 703–709
18. Hori, T., Osaka, F., Chiba, T., Miyamoto, C., Okabayashi, K., Shimbara, N., Kato, S., and Tanaka, K. (1999) *Oncogene* **18,** 6829–6834
19. Hochstrasser, M. (2000) *Science* **5479,** 563–564
20. Kamura, T., Conrad, M. N., Yan, Q., Conaway, R. C., and Conaway, J. W. (1999b) *Genes Dev.* **13,** 2928–2933
21. Ruegger, M., Dewey, E., Gray, W. M., Hobbie, L., Turner, J., and Estelle, M. (1998) *Genes Dev.* **12,** 198–207
22. Xie, D.-X., Feys, B. F., James, S., Nieto-Rostro, M., and Turner, J. G. (1998) *Science* **280,** 1091–1094
23. del Pozo, J. C., and Estelle, M. (1999) *Trends Plant Sci.* **4,** 107–112
24. del Pozo, J. C., and Estelle, M. (2000) *Plant Mol. Biol.* **44,** 123–128
25. McCarty, D. R., and Chory, J. (2000) *Cell* **103,** 201–209
26. Gray, W. M., Kepinski, S., Rouse, D., Leyser, O., and Estelle, M. (2001) *Nature*

414, 271–276
27. Samach, A., Klenz, J. E., Kohalmi, S. E., Risseeuw, E., Haughn, G. W., and Crosby, W. L. (1999) *Plant J.* **20,** 433–445
28. Nelson, D. C., Lasswell, J., Rogg, L. E., Cohen, M. A., and Bartel, B. (2000) *Cell* **101,** 331–340
29. Somers, D. E., Schultz, T. F., Milnamow, M., and Kay, S. A. (2000) *Cell* **101,** 319–329
30. Schultz, T. F., Kiyosue, T., Yanovsky, M., Wada, M., and Kay, S. A. (2001) *Plant Cell* **13,** 2659–2670
31. Dieterle, M., Zhou, Y.-C., Schäfer, E., Funk, M., and Kretsch, T. (2001) *Genes Dev.* **15,** 939–944
32. Woo, H. R., Chung, K. M., Park, J.-H., Oh, S. A., Ahn, T., Hong, S. H., Jang, S. K., and Nam, H. G. (2001) *Plant Cell* **13,** 1779–1790
33. Kim, H. S., and Delaney, T. P. (2002) *Plant Cell* **14,** 1469–1482
34. Gagne, J. M., Downes, B. P., Shiu, S. H., Durski, A. M., and Vierstra, R. D. (2002) *Proc. Natl. Acad. Sci. U. S. A.* **99,** 11519–11524
35. Sambrook, J., Fritsch, E. F., and Maniatis, T. (1989). *Molecular Cloning: A Laboratory Manual*, 2nd Ed., Cold Spring Harbor Laboratory, Cold Spring Harbor, NY
36. Ausubel, F. M., Brent, R., Kingston, R. E., Moore, D. D., Seidman, J. G., Smith, J. A., and Struhl, K. (eds) (1994). *Current Protocols in Molecular Biology*, Greene Publishing, New York
37. Criqui, M. C., Parmentier, Y., Derevier, A., Shen, W.-H., Dong, A., and Genschik, P. (2000) *Plant J.* **24,** 763–773
38. Aoyama, T., and Chua, N. H. (1997) *Plant J.* **11,** 605–612
39. Bechtold, N., Ellis, J., and Pelletier, G. (1993) *C. R. Acad. Sci. Ser. III Sci. Vie* **316,** 1194–1199
40. Clough, S. J., and Bent, A. F. (1998) *Plant J.* **16,** 735–743
41. Gil, P., Liu, Y., Orbovic, V., Verkamp, E., Poff, K. L., and Green, P. J. (1994) *Plant Physiol.* **104,** 777–784
42. Genschik, P., Jamet, E., Philipps, G., Parmentier, Y., Gigot, C., and Fleck, J. (1994) *Plant J.* **6,** 537–546
43. Chaboute, M. E., Chaubet, N., Philipps, G., Ehling, M., and Gigot, C. (1987) *Plant Mol. Biol.* **8,** 179–191
44. Storozhenko, S., De Pauw, P., Kushnir, S., Van Montagu, M., and Inze, D. (1996) *FEBS Lett.* **390,** 113–118
45. Shen, W. H., Parmentier, Y., Hellmann, H., Lechner, L., Dong, A., Masson, J., Granier, F., Lepiniec, L., Estelle, M., and Genschik, P. (2002) *Mol. Biol. Cell* **13,** 1916–1928
46. Hamilton, A. J., and Baulcombe, D. C. (1999) *Science* **286,** 950–952
47. Healy, J. M., Menges, M., Doonan, J. H., and Murray, J. A. (2001) *J. Biol. Chem.* **276,** 7041–7047
48. Guthrie, C., and Fink, G. R. (1991) *Methods Enzymol.* **194,** 795–823
49. Lechner, E., Goloubinoff, P., Genschik, P., and Shen, W. H. (2002) *Gene* (*Amst.*) **290,** 63–71
50. Chen, A., Wu, K., Fuchs, S. Y., Tan, P., Gomez, C., and Pan, Z. Q. (2000) *J. Biol. Chem.* **275,** 15432–15439
51. del Pozo, J. C., and Estelle, M. (1999) *Proc. Natl. Acad. Sci. U. S. A.* **96,** 15342–15347
52. Dharmasiri, S., and Estelle, M. (2002) *Plant Mol. Biol.* **49,** 401–409
53. Leyser, O. (2001) *Curr. Opin. Plant Biol.* **4,** 382–386
54. Kang, H. G., Fang, Y., and Singh, K. B. (1999) *Plant J.* **20,** 127–133
55. Penninckx, I. A., Eggermont, K., Terras, F. R., Thomma, B. P., De Samblanx, G. W., Buchala, A., Metraux, J. P., Manners, J. M., and Broekaert, W. F. (1996) *Plant Cell* **8,** 2309–2323
56. Vaucheret, H., Beclin, C., and Fagard, M. (2001) *J. Cell Sci.* **114,** 3083–3091
57. Voinnet, O. (2001) *Trends Genet.* **17,** 449–459
58. Bachmair, A., Novatchkova, M., Potuschak, T., and Eisenhaber, F. (2001) *Trends Plant Sci.* **6,** 463–470
59. Yu, Z. K., Gervais, J. L., and Zhang, H. (1998) *Proc. Natl. Acad. Sci. U. S. A.* **95,** 11324–11329
60. Maeda, I., Ohta, T., Koizumi, H., and Fukuda, M. (2001) *FEBS Lett.* **494,** 181–185
61. Riou-Khamlichi, C., Huntley, R., Jacqmard, A., and Murray, J. A. (1999) *Science* **283,** 1541–1544
62. Riou-Khamlichi, C., Menges, M., Healy, J. M., and Murray, J. A. (2000) *Mol. Cell. Biol.* **20,** 4513–4521
63. Zhao, D., Yang, M., Solava, J., and Ma, H. (1999) *Dev. Genet.* **25,** 209–223
64. Yang, M., Hu, Y., Lodhi, M., McCombie, R., and Ma, H. (1999) *Proc. Natl. Acad. Sci. U. S. A.* **96,** 11416–11421
65. Gray, W. M., del Pozo, J. C., Walker, L., Hobbie, L., Risseeuw, E., Banks, T., Crosby, W. L., Yang, M., Ma, H., and Estelle, M. (1999) *Genes Dev.* **13,** 1678–1691
66. Gray, W. M., Hellmann, H., Dharmasiri, S., and Estelle, M. (2002) *Plant Cell* **14,** 2137–2144
67. Xu, L., Liu, F., Lechner, E., Genschik, P., Crosby, W. L., Ma, H., Peng, W., Huang, D., and Xie, D.-X. (2002) *Plant Cell* **14,** 1919–1935
68. Leyser, H. M., Lincoln, C. A., Timpte, C., Lammer, D., Turner, J., and Estelle, M. (1993) *Nature* **364,** 161–164
69. Harper, J. W., and Elledge, S. J. (1999) *Nat. Cell Biol.* **1,** E5–E7
70. Vandepoele, K., Raes, J., De Veylder, L., Rouze, P., Rombauts, S., and Inze, D. (2002) *Plant Cell* **14,** 903–916
71. Ivan, M., and Kaelin, W. G. (2001) *Curr. Opin. Genet. Dev.* **11,** 27–34